Available online at www.sciencedirect.com
ScienceDirect
Physics Procedia 12 (2011) 323–329
Physics Procedia

# Laser Cladding of Ti-6Al-4V Powder on Ti-6Al-4V Substrate: Effect of Laser Cladding Parameters on Microstructure

Ryan Cottam[ac] *and Milan Brandt[bc]

[a] Industrial Laser Applications Laboratory, IRIS, Faculty of Engineering and Industrial Sciences, Swinburne University of Technology, Victoria, Australia
[b]School of Aerospace, Mechanical and Manufacturing Engineering, RMIT University, Bundoora, Victoria, 3083, Australia
[c]Defence Materials Technology Centre, Victoria, Australia

**Abstract**

The laser cladding of Ti-6Al-4V powder on Ti-6Al-4V substrate has been investigated to determine laser parameters that could be used as a repair technology for Ti-6Al-4V components. The parameters chosen for the investigation were developed by an analytical laser cladding model. Holding clad height and melt pool depth constant, the traversing speed was varied between 300mm/min and 1500mm/min, an associated power for the given speed was calculated by the model. Two different melt pool depths were used in the calculation of laser power for a given process velocity. The resulting microstructures in the clad zone varied from a relatively thin martensitic structure to a dendritic/thick martensitic structure. The heat affected zone (HAZ) showed a refinement of the Widmanstatten microstructure with a decreasing laser traversing speed and a coarser martensitic structure for the sample prepared with a deeper melt pool.

*Keywords:* Laser Cladding; Ti-6Al-4V; Microstructres

## 1. Introduction

Current and next generation aircraft used by the Australian defence forces have many components made from Ti alloys and in particular Ti-6Al-4V. Many of these components suffer from wear or foreign object damage. A repair technique that could restore such components would yield significant savings for the Australian defence forces. Laser cladding is a process that offers the potential to develop such a repair technology. The process has been used to repair a blisk blades made from Ti6242 [1], but the details of the laser processing parameters were not given. There has also been work on the building of 3D structures for direct manufacture [2-4]. Laser processing parameters have been varied in these studies but not to a great extent. Therefore an investigation into the effect of cladding parameters when cladding Ti-6Al-4V is required to optimize the process.

The main parameters of laser cladding are: laser traversing speed, laser power, laser spot size, laser profile, and powder feed rate. Potentially different combinations of these parameters can produce the same clad dimension. Based on this approach this investigation used an analytical cladding model to predict combinations of laser cladding parameters that would produce a clad of 1mm thickness at different laser traversing speeds and two

* Corresponding author. Tel.: +61 3 92144878.
*E-mail address*: rcottam@swin.edu.au.


doi:10.1016/j.phpro.2011.03.041

different melt pool depths. This is a new approach to laser cladding research and will potentially yield the optimum cladding parameters for cladding Ti-6Al-4V powder on Ti-6Al-4V substrate.

## 2. Experimental

Laser cladding was conducted with a 2.5kW fibre delivered Nd:YAG laser and side injecting powder nozzle. The Ti-6Al-4V plate used as the substrate for the cladding was 6mm thick, 210x115mm in area and was in the annealed condition, Figure 1. The titanium powder used to create the clad layer was supplied by TLS and had an average particle size of 60μm. Table 1 shows the laser parameters used to produce the 6 specimens. These parameters were chosen based on the results of an analytical cladding model, the detail of which are being presented elsewhere. As Table 1 shows there are duplicates in laser traversing speed. For the second set of traversing speeds a higher laser power was used to increase the penetration of the melt pool into the substrate and hence evaluate its effect on the clad produced. A 3mm diameter Gaussian shaped laser spot was used by the model and the experiment. Pads of 25x25mm were produced using an inter-tack spacing of 0.5mm.

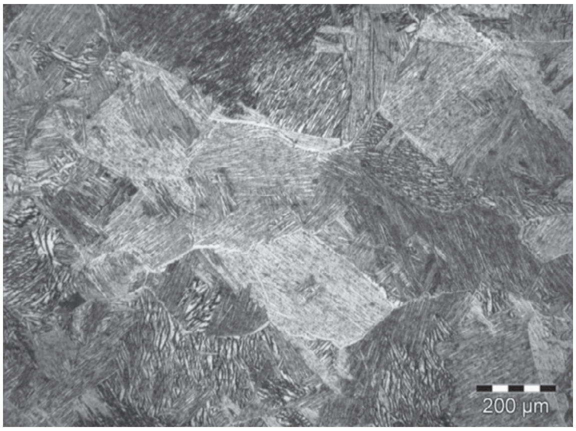


Figure 1. Substrate microstructure

Table 1. Laser cladding parameters

| **Sample Designation** | **Traversing Speed** (mm/min) | **Laser Power** (W) | **Powder Feed Rate** (g/min) |
|---|---|---|---|
| Condition 1 | 1500 | 862 | 6.6 |
| Condition 2 | 600 | 616 | 2.64 |
| Condition 3 | 300 | 456 | 1.32 |
| Condition 4 | 1500 | 1477 | 6.6 |
| Condition 5 | 600 | 885 | 2.64 |
| Condition 6 | 300 | 686 | 1.32 |

After cladding the specimens were cut transverse to the clad direction using electro-discharge machining. The samples were then mounted, ground, polished and etched. 2% HF, swabbed on the surface for 30 second was the procedure used to etch the samples.

Further analysis of the microstructure of conditions 6 was carried out using scanning electron microscopy (SEM), X-ray diffraction (XRD) and microhardness measurements. SEM was conducted on a field emission Zeiss 40VP supra microscope fitted with and INCA X-ray detector. Hardness tests were carried out on a Buehler microhardness tester with a load of 300g. XRD was carried out with a scan step of $0.05^{o}$ 2θ and a count time of 2s.

## 3. Results and Discussion

### *3.1. Clad zone microstructures*

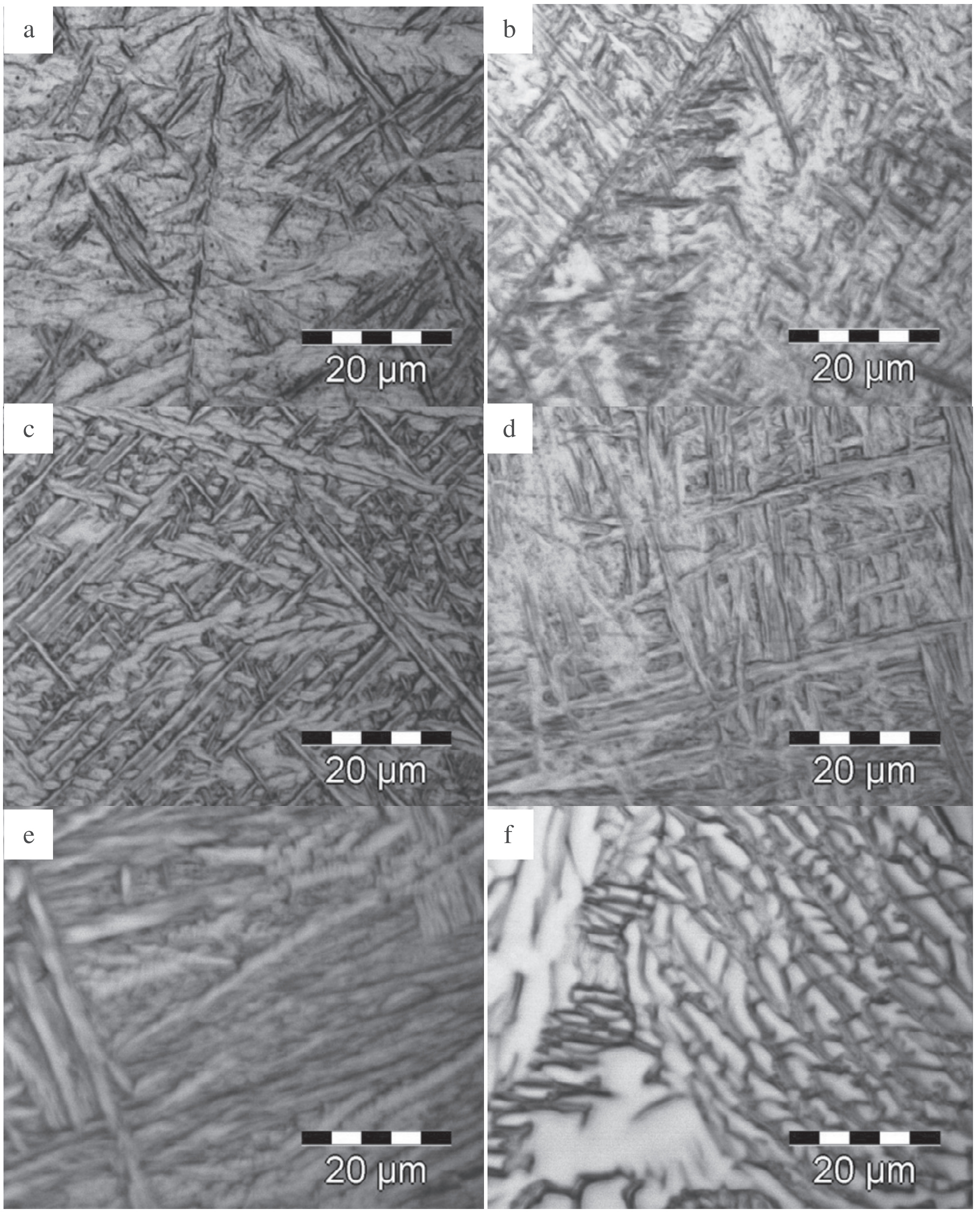


Figure 2 . Microstructures of the clad region; a-condition 1; b-condition 2; c-condition 3; d-condition 4; e-condition 5; f-condition 6.

Figure 2 shows the microstructures in the clad zone as a result of the six laser processing conditions. For conditions 1-3 (Figure 2 a-c) the melt pool depth was the same but the laser traversing speed was decreasing. Visually it appears the martensite laths, $\alpha$', in the three micrographs are increasing in thickness as the laser traversing speed decreases, which is indicative of the decreasing cooling rate. For conditions 4-6 (Figure 2 d-f) with a deeper melt pool (higher laser power) martensite is observed as well but is much thicker than that for conditions 1-3. This martensite might be the $\alpha$ massive phase reported by Ahmed *et al* [5]. Interestingly Figure 2f, the slowest traversing speed and the largest laser power, appears to have dendrites in a matrix of thick martensite, both features are indicative of a slow cooling rate. This type of microstructure is unique compared with the literature and further analysis was performed to identify its character and is addressed later in the paper.

*3.2. Heat affected zone microstructures*

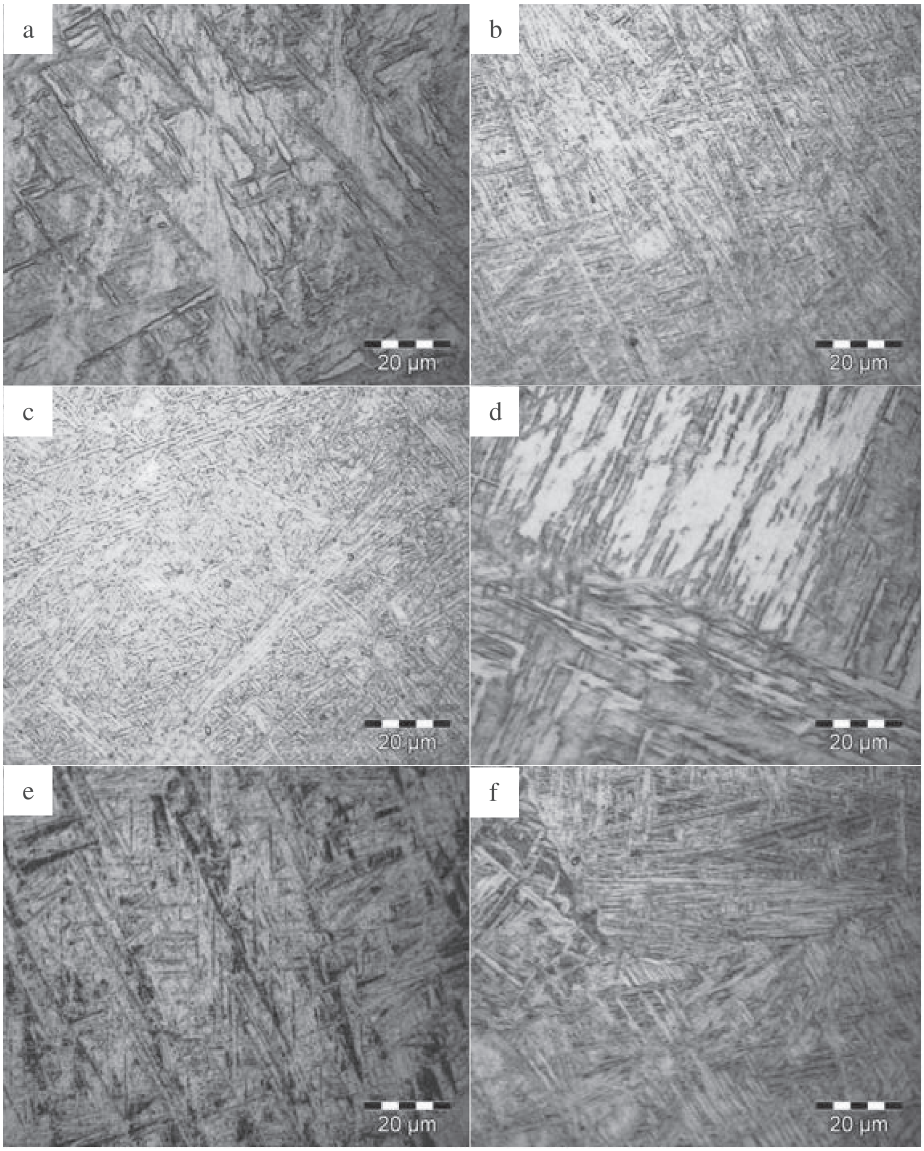


Figure 3. Microstructures of the HAZ region; a-condition 1; b-condition 2; c-condition 3; d-condition 4; e-condition 5; f-condition 6.

Widmanstatten, $\alpha$, forms in the HAZ due to the process conditions, Figure 3. The temperature in the heat affected zone must have exceeded the $\beta$ transus temperature of 994°C [5] and then cooled fast enough to form the fine Widmanstatten structure, which is consistent with the findings of Kobryn [2]. Unlike the clad zone the HAZ shows a refinement in the lath thickness with decreasing laser processing speed, Figure 1 a-c. This suggests that the cooling rate in the HAZ is increasing with a decrease in the laser processing speed. This trend is also evident for conditions producing the deeper melt pool, conditions 4-6 (Figure 3 d-f). The thickness of the Widmanstatten laths for conditions 4-6 is greater than that for the equivalent speed but lower laser power conditions 1-3,( Figure 3 a-c ) and can be attributed to a greater heat input. Finite element modeling of laser parameters used in this investigation to determine the rate of heating and cooling at different regions in the clad may elucidate why the Widmanstatten in the HAZ decreases in thickness with a decrease in traversing speed and the clad zone martensite increases in thickness with decreasing speed.

### *3.3. Analysis of condition 6 microstructure*

The microstructure in the clad region produced as a result of processing using condition 6 is different to that reported in the literature for the cladding Ti-6Al-4V. The low magnification picture of this region, Figure 3a, shows that there are regions that look like dendrites surrounded by a matrix of thick martensite. Microhardness measurements of the clad zone, Figure 4b and Figure 5, show that the dendrite is much lower in hardness (500HV) than the martensite (600HV).

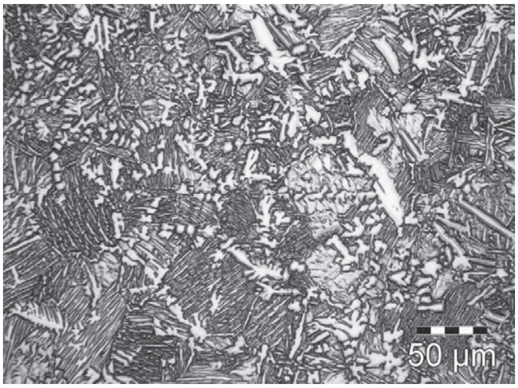


a

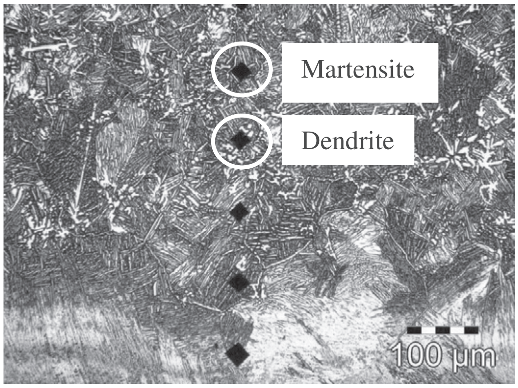


b

Figure 4. Optical micrographs of the clad region of clad produced by condition 6; a – low magnification; b – image showing hardness impression

XRD was performed to identify if any new phase(s) had formed as a result of the cladding or if there was more retained $\beta$ in the microstructure. The results of the XRD, Figure 6, show that no new peaks were present and that all the peaks for the substrate and the clad are coincident indicating that crystallography of the two materials is similar. As the labeling of the peaks shows both areas of the clad are predominantly $\alpha$ (larger peaks) with small amount of $\beta$.

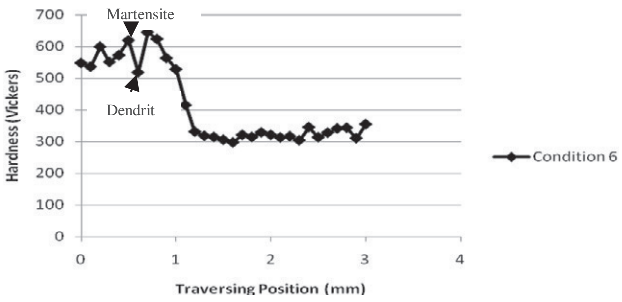


Figure 5. Microhardness traverse of clad layer produced by condition 6

To identify any segregation of the alloying elements X-ray mapping of the clad region of condition 6 was performed and is shown in Figure 7. These maps show no distinct segregation as a result of solidification during processing. Typically segregation occurs as a result of dendrite formation and depends on the phase diagram and the size of the liquid-solid phase region. Reference to the phase diagram for Ti-6Al-4V [6] shows that this region is only small and so not much segregation would be expected.

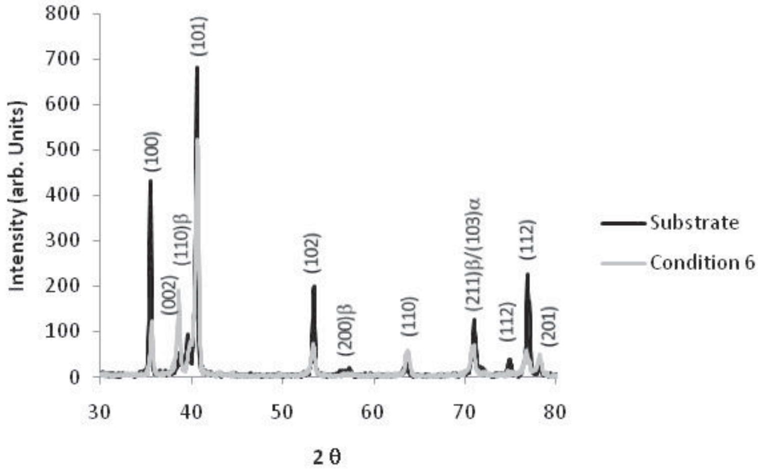


Figure 6. XRD 2θ scan showing the intensities for both the substrate and clad zone.

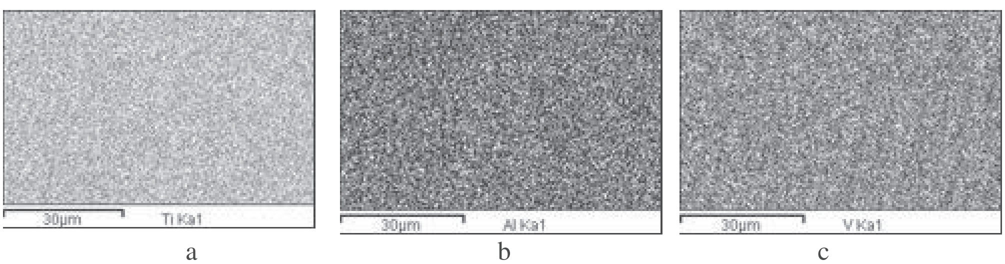


Figure 7. X-ray maps produced by SEM of the clad region produced by condition 6; a – titanium; b – aluminum; c – vanadium.

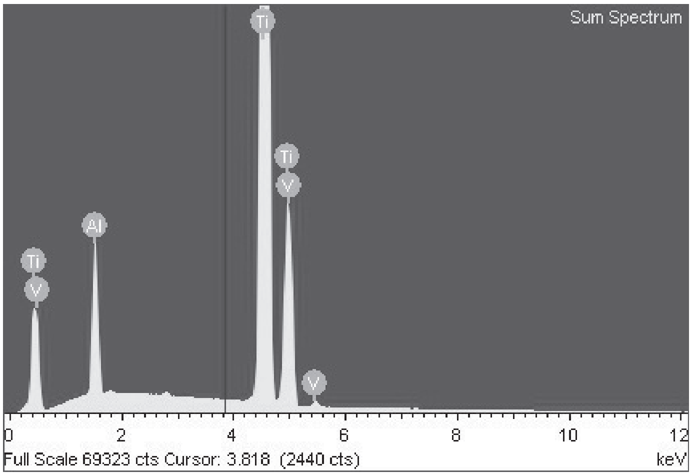


Figure 8. X-ray spectrum analysis from SEM.

Even though no new phases were identified one of the problems with processing Ti-6Al-4V is oxygen and nitrogen absorption above 500$^{o}$C. Processing was carried out in a chamber filled with argon coupled with the argon shielding gas of the laser. The X-ray spectrum, Figure 7, shows no evidence for oxygen or nitrogen in the structure. This is evidence that the shielding of the cladding was adequate.

Given that what appears to be dendrites are softer than the matrix of martensite, and that there is no new phase in the XRD diffraction spectrum observed, the clad microstructure of condition 6 is dendrites of $\alpha$ in a matrix of $\alpha$'martensite which is quite thick and may be the $\alpha$ massive phase.

## 4. Conclusions

Martensite, $\alpha$', forms in the clad and a fine Widmanstatten in the HAZ due to laser cladding of Ti-6Al-4V powder on Ti-6Al-4V substrate. For the slowest laser traversing speed and highest power used in this study, a microstructure of dendrites and martensite forms due to the slow cooling rate of this set of conditions. The degree of refinements of the Widmanstatten in the HAZ due to a decrease in laser traversing speed and increase in the martensite thickness in the clad zone due to a decrease in the laser traversing speed needs finite element modeling of the heating and cooling cycle to be conducted to verify the differences.

## Acknowledgements

This work has been conducted for the Defence Material Technology Centre (DMTC) as part of project 4.1 'Repair Technologies for Current and Next Generation Aircraft Systems'. The authors would like to thanks Mr. Girish Thipperudrappa for his assistance with laser deposition experiments.

## References

[1] Richter, K.H., S. Orban, and S. Nowotny: Laser cladding of the titanium alloy Ti6242 to restore damaged blades. In Proceedings of the 23rd international congress on applications of lasers and electro-optics. (2004)

[2] Kobryn, P.A., E.H. Moore, and S.L. Semiatin: The effect of laser power and traverse speed on microstructure, porosity, and build height in laser-deposited Ti-6Al-4V. In: Scripta Materialia, 43 (2000) 299-305.

[3] Meacock, C. and R. Vilar: Laser powder microdeposition of CP2 Titanium. In: Materials and Design 29 (2008) 353-361.

[4] Wu, X., J. Liang, J. Mei, C. Mitchell, P.S. Goodwin, W. Voice: Microstrucutres of laser-deposited Ti-6Al-4V In: Materials and Design, 25 (2004) 137-144.

[5] Ahmed, T. and J. Rack: Phase transformations during cooling in alpha + beta titanium alloys. In: Materials Science and Engineering A 243 1998 206-211.

[6] Donachie, M.J: Titanium: a technical guide. 2nd ed., Ohio, ASM International (2000)